to be published in the *Astrophysical Journal Letters*

Chandra Limits on X-ray Emission Associated with the Supermassive Black Holes in Three Giant Elliptical Galaxies

Michael Loewenstein[1], Richard F. Mushotzky, Lorella Angelini[2], Keith A. Arnaud[1]

Laboratory for High Energy Astrophysics, NASA/GSFC, Code 662, Greenbelt, MD 20771

loew@larmes.gsfc.nasa.gov

and

Eliot Quataert

Institute for Advanced Study, School of Natural Sciences, Einstein Drive, Princeton, NJ 08540

eliot@ias.edu

ABSTRACT

Elliptical galaxy nuclei are the sites of the largest black holes known, but typically show little or no nuclear activity. We investigate this extreme quiescence using *Chandra X-ray Observatory* observations of the giant elliptical galaxies NGC 1399, NGC 4472, and NGC 4636. The unique *Chandra* imaging power enables us to place upper limits of 7.3, 15 and 28×10^{-9} the Eddington luminosity for the $\sim 10^8 - 10^9$ $M_\odot$ black holes in NGC 1399, NGC 4472, and NGC 4636, respectively. The corresponding radiative efficiencies in this band are 4.1, 24, and 620×10^{-6} using Bondi accretion rates derived from the *Chandra* hot interstellar gas surface brightness profiles. These limits are inconsistent with basic advection-dominated accretion flow (ADAF) models for NGC 1399 and NGC 4472, indicating accretion onto the black hole at $\lesssim 10\%$ of the Bondi rate.

Subject headings: accretion, accretion disks — black hole physics — galaxies: elliptical and lenticular — galaxies: nuclei — X-rays: galaxies

[1]Also with the University of Maryland Department of Astronomy

[2]Also with the Universities Space Research Association

1. Introduction

Knowledge about the frequency and masses of supermassive black holes (SMBH) in galactic nuclei, and the characteristics of their associated radiation, deepen our understanding of galaxy formation and clarify its connection with the active galactic nuclei (AGN) phenomenon (e.g., Blandford 1999). While the intense energetics and rapid variability in the most luminous active galaxies form the empirical foundation of the SMBH/AGN paradigm, such extreme objects are rare – especially in the local universe.

Nevertheless, there is now a consensus that most, if not all, galaxies host SMBH. This is based, in part, on the high frequency of low-level nuclear activity in nearby galaxies (Ho, Filipenko, & Sargent 1997), and on statistical arguments connected to the cosmic X-ray background (e.g., Fabian & Iwasawa 1999). However, the strongest evidence for the ubiquity of SMBH comes from dynamical studies. Magorrian et al. (1998) found that, of 32 galaxies that could be fit with an axisymmetric dynamical model, 26 (29) require the presence of a central massive ($\sim 10^8 - 10^{10}$ $M_\odot$) dark object at 95% (68%) confidence. More unambiguous and accurate measurements based on *Hubble Space Telescope* (*HST*) stellar or ionized gas spectroscopy confirms the presence of SMBH while deriving systematically lower SMBH masses (Gebhardt et al. 2000a; Merritt & Ferrarese 2001a).

Although kinematically-studied luminous AGN are found to host SMBH (Gebhardt et al. 2000b; McLure & Dunlop 2000), the converse is not true: activity in most SMBH host galaxies is modest or absent. This can be quantified by considering the ratio of the nuclear luminosity to the Eddington luminosity ($L_{\rm edd} = 1.25\ 10^{38} M_{\rm SMBH}$, where the black hole mass $M_{\rm SMBH}$ is measured in solar units). The most powerful AGN have ratios on the order of unity, as expected from the theory of thin disks accreting at their maximal rate. However, this ratio is less than 10^{-7} and 10^{-4}, respectively, in the two most securely measured SMBH – SgrA* at the Galactic Center (Quataert, Narayan, & Reid 1999) and NGC 4258 (Gammie, Narayan, & Blandford 1999). If these SMBH accrete at the Bondi (1952) rate, they must do so in a fundamentally different – and much less radiatively efficient – way than in luminous AGN. The theory of advection-dominated accretion flows (ADAF; e.g., Narayan & Yi 1994), provides a predictive formalism for explaining the observed quiescence in the nuclei of SgrA*, NGC 4258, and other systems (Fabian & Rees 1995; Mahadevan 1997).

Elliptical galaxies are the sites of the most luminous quasars, and also host the most extreme cases of quiescent SMBH. Although they contain nuclear black holes with the highest estimated masses and are observed to contain an ample supply of fuel in the form of X-ray emitting hot interstellar gas, they often emit less than $10^{-6} L_{\rm edd}$ (Loewenstein et al. 1998; Di Matteo et al. 2000). Radio/X-ray observations of some systems are inconsistent with predictions of the simplest models of an ADAF accreting at the Bondi rate, but can be

accommodated by variations that include outflow (Blandford & Begelman 1999; Quataert & Narayan 1999; Di Matteo et al. 1999) or convection (Narayan, Igumenshchev, & Abramowicz 2000; Quataert & Gruzinov 2000).

Prior to the launch of the *Chandra X-ray Observatory*, X-ray searches for nuclear point sources in elliptical galaxies were complicated in the imaging domain by centrally concentrated hot gas that dominates the soft X-ray flux; and, in the spectral domain by an extended hard component consisting of X-ray binaries. Thus the previous sensitivity to SMBH-associated X-ray emission, for even the nearest giant ellipticals, was $\sim 10^{40}$ erg s^{-1} (Roberts & Warwick 2000; Sulkanen & Bregman 2001), as neither the *ASCA* SIS/GIS nor the *ROSAT* PSPC/HRI had the necessary combination of sensitivity and spatial and spectral resolution to probe more deeply. Allen, Di Matteo, & Fabian (2000) claim to detect a very hard nuclear X-ray component in six elliptical galaxies with characteristics consistent with ADAF/outflow models, given the observed radio emission (Di Matteo et al. 1999). However, these results are based on a non-unique decomposition of *ASCA* spectra.

Because of the presence of bright stellar cores and dust, the best approach for constraining the level of SMBH activity is via high angular resolution X-ray observations (e.g., George et al. 2001): for a typical AGN X-ray/optical ratio, the *Chandra* detection threshold corresponds to a B magnitude ~ 24, while elliptical galaxy central surface brightnesses range from $\sim 11 - 16$ mag arcsec^{-2}. This is further demonstrated by deep *Chandra* surveys in combination with optical follow-up. Low-luminosity AGN, most not optically detected, dominate the X-ray background; and, nonthermal emission is found to be common – at any given time $\sim 10\%$ of all bright galaxies host $L_X \gtrsim 10^{41}$ erg s^{-1} AGN (Mushotzky et al. 2000; Barger et al. 2001). There is also a high frequency of nuclear X-ray point sources associated with local AGN, though often at levels that overlap in luminosity with X-ray binaries (Ho et al. 2001). *Chandra* has detected unresolved nuclear emission associated with quiescent SMBH in M31 at $\sim 5 \times 10^{-9} L_{\rm edd}$ (Garcia et al. 2000), the Galactic Center at $\sim 10^{-11} L_{\rm edd}$ (Baganoff et al. 2001), and NGC 6166 at $\sim 10^{-7} L_{\rm edd}$ (Di Matteo et al. 2001).

In this paper we use *Chandra* imaging data to place luminosity limits on any nuclear point sources in the elliptical galaxies NGC 1399, NGC 4472, and NGC 4636. These limits raise new questions about the radiative efficiency and rate of accretion onto supermassive black holes. Following Merritt & Ferrarese (2001b), we adopt distances of 20.5, 16.7, and 15.0 Mpc for NGC 1399, NGC 4472, and NGC 4636, respectively.

2. Data Analysis and Results

2.1. Observations, Data Reduction and Analysis

NGC 1399, NGC 4472, and NGC 4636 were observed with the *Chandra* ACIS-S detector for 40–60 ksec during Cycle 1. Results on the diffuse hot gas emission and the X-ray binary population, and a more detailed data reduction description, are included elsewhere (e.g, Angelini, Loewenstein, & Mushotzky 2001). The latest revised standard pipeline processing was used for NGC 4472 and NGC 4636, while an earlier version in combination with additional bad pixel removal, gain map correction, and quantum efficiency map correction was used for NGC 1399. Final useful exposure times are 56, 40, and 52 ksec for NGC 1399, NGC 4472, and NGC 4636, respectively. NGC 1399 was approximately centered on the S3 chip; NGC 4636 and NGC 4472 were positioned at the standard ACIS-S aimpoint. 1.25–7 keV images of the central $50'' \times 50''$ are shown for all three galaxies in Figures 1a, 1b, and 1c. The positions of the optical nuclei from archival *HST* NICMOS (NGC 4472, NGC 4636) or WFPC2 (NGC 1399) images are marked. The brightest point sources in the images are easily visible and indicated in the images; their counting rates are in the 0.005–0.008 cts s^{-1} range. The bright X-ray core in NGC 4472 is resolved and has a thermal spectrum. Only in the case of NGC 4636 is there a possible coincidence of the nucleus with a *Chandra* X-ray source (just to the southwest of the nuclear position indicated in Figure 1c), with a 0.3–7 keV count rate ~ 0.004 cts s^{-1} (see below). 0.3–7.0 keV surface brightness profiles are shown in Figure 2. For illustration purposes, the NGC 4636 profile is centered on the near-nuclear source. No excess emission from unresolved nuclear emission is apparent for the other two galaxies.

The position of the nucleus in NGC 1399 is identified based on registration of globular cluster X-ray sources with their WFPC2 counterparts (Angelini et al. 2001); the resulting *HST* and *Chandra* centroids are consistent. Similarly, the nucleus of NGC 4636 is located based on registration with a bright NICMOS source and with the USNO catalog (Monet et al. 1998), and is found *not* to be consistent with the position of the near-nuclear source (Figure 1c). For NGC 4472, we adopt the unregistered *HST* centroid that is consistent with the peak in the soft thermal emission seen in the broadband *Chandra* image (Figure 1b). 3σ upper limits to any nuclear X-ray point source emission are derived following Gehrels (1986). Counts are accumulated in inner ("source") and outer ("background") concentric annuli with radii that are varied to obtain the tightest upper limit. The *Chandra* calibration database enclosed energy function at the appropriate off-axis angle is used, and an exposure map correction is applied for NGC 1399, which was centered off-axis. The assumed position of the SMBH is allowed to vary in a $3'' \times 3''$ box (corresponding to a very conservative adopted *Chandra*/*HST* relative systematic pointing uncertainty) centered on the assumed

nuclear positions and the highest upper limit in this box is adopted. These boxes encompass the peaks of the diffuse emission for NGC 4472 and NGC 1399. The diffuse hot gas emission is implicitly assumed to be locally flat on average when treated as "background", consistent with the flat central surface brightness profiles (Figure 2). Luminosity upper limits are derived both in the 0.3–7 keV and 2–10 keV energy bands assuming a slope 1.5 power-law spectrum – the limits increase by ~ 2 for slope 0.5. Due to reduced dilution from the diffuse hot gas emission, the 2–10 keV count rate limits are 3–5 times lower than in the softer band; however, because of the declining effective area the energy flux upper limits are comparable. The 0.3–7 keV detection limit varies from a few 10^{37} erg s^{-1} in regions of low surface brightness hot ISM emission to a few 10^{38} erg s^{-1} in the core of NGC 1399.

The 2–10 keV limits – all derived within $1''$ of the optical nucleus – are displayed in Table 1; these correspond to 28, 23, and 16 counts for NGC 1399, NGC 4472, and NGC 4636, respectively – comparable to the brightest sources in the subimages shown in Figure 1. Table 1 also includes less conservative, but perhaps more realistic, limits calculated by fixing the positions at the assumed nuclear positions described above.

The inner gas density profile is estimated by fitting the point-source-subtracted surface brightness profiles with β-models,

$$\Sigma = \Sigma_o \left(1 + \frac{r^2}{a^2}\right)^{-(3\beta-1/2)} \tag{1}$$

out to some maximum radius, followed by analytical deprojection with conversions obtained from spectral fits to the inner regions (best-fit temperatures $kT = 0.8$, 0.8, and 0.6 keV for NGC 1399, NGC 4472, and NGC 4636, respectively). The quality of fit declines as the maximum radius is increased due to deviations from the β-model, but the profiles are sufficiently concentrated that the central density estimates – 4.6, 3.2, and 1.1×10^{-25} gm cm^{-3} for NGC 1399, NGC 4472, and NGC 4636, respectively – are robust.

2.2. Accretion Rates and Eddington Ratio Limits

Individual black hole masses for the three galaxies studied here have been estimated by Magorrian et al. (1998) from two-integral dynamical modeling of ground-based kinematical data. A more accurate value can be derived using the correlation with bulge velocity dispersion, σ, derived for galaxies with limits based on *HST* spectroscopy. Therefore, we adopt SMBH masses from Merritt & Ferrarese (2001b) (Table 1); these are 3–5 times lower than in Magorrian et al. (1998). The resulting 2–10 keV luminosities in units of the Eddington luminosity and the Bondi (1952) accretion rates for adiabatic spherical inflow are displayed

in Table 1. Our derived upper limits on $L_X/L_{\rm edd}$ are 7.3×10^{-9}, 1.5×10^{-8}, and 2.8×10^{-8} for NGC 1399, NGC 4472, and NGC 4636, respectively. The corresponding efficiencies, assuming accretion at the Bondi rate $\dot{M}_{\rm Bondi}$, are 4.1×10^{-6}, 2.4×10^{-5}, and 6.2×10^{-4}.

3. The Nature of the Accretion Flow

The conservative upper limits we derive are 1–2 orders of magnitude lower than the luminosities estimated by Allen et al. (2000) using *ASCA* spectral decomposition. Direct *Chandra* images (Angelini et al. 2001) indicate that most of the hard X-ray emission spatially unresolved by *ASCA* originates in X-ray binaries. Since upper limits on the nuclear X-ray emission and estimates of the Bondi accretion rate have each decreased by $\sim 10-30$ from Di Matteo et al. (2000) (the latter because of lower black hole mass estimates)[3], a re-examination of the nature of the accretion flow is in order.

For our estimated black hole masses and Bondi accretion rates, we have computed spectra using the techniques described in Quataert & Narayan (1999); we aim to test the basic ADAF model and so do not include outflows or convection. The resulting predicted 2–10 keV luminosities, $L_{\rm ADAF}$, are $\approx 2\times10^{41}$, 10^{40}, and 10^{36} ergs s^{-1} for NGC 1399, NGC 4472, and NGC 4636, respectively (Table 1). Our observational upper limits are thus significantly below the ADAF predictions for NGC 1399 and NGC 4472, but consistent for NGC 4636. The predicted X-ray luminosities in the standard ADAF models for the cases of NGC 1399 and NGC 4472 are dominated by Compton scattered synchrotron emission that originates close to the black hole. The luminosity is primarily sensitive to the gas density (i.e., accretion rate) and electron temperature. A factor of ~ 10 decrease in the accretion rate below the Bondi value can reduce the predicted luminosity to the observational limits.

With the revised black hole masses and accretion rates we find that the radio flux predicted by the ADAF model is less than the observed flux for NGC 1399 and NGC 4636, but is in excess for NGC 4472; thus the radio flux problem highlighted by Di Matteo et al. (1999) is somewhat ameliorated. Finally, a preliminary *HST* measurement of the nuclear FUV emission in NGC 1399 (0'Connell et al., in preparation), – $\nu L_\nu \sim 7\ 10^{38}$ erg s^{-1} – also conflicts with pure-inflow ADAF models, although dust may be an issue at this wavelength.

Our observations require a modification of the standard ADAF/Bondi model such that

[3]For NGC 4636 our Bondi accretion rate is ≈ 3000 times smaller than that of Di Matteo et al. (2000). A factor of ≈ 10 is due to our smaller black hole mass; the remainder is primarily due to a lower inferred central gas density that may be underestimated since the accretion radius is unresolved in this case.

the gas density near the SMBH is reduced by at least a factor of ~ 10. This could be due to the role of strong outflows or convection in an ADAF. Alternatively, the central regions of these galaxies may not be in steady state due to heating by supernovae or by episodic accretion onto the central SMBH (e.g., Ciotti & Ostriker 1997). In addition the cooling time at the accretion radius $R_{\rm Bondi}$ (Table 1) is $< 10^7$ yr for all three galaxies; so, inflow with mass deposition could be important (Brighenti & Mathews 1999).

4. Conclusions

We have used *Chandra* observations to place new and unprecedented upper limits on the X-ray emission associated with $\sim 10^8 - 10^9$ $M_\odot$ nuclear black holes in three giant elliptical galaxies. The black holes clearly are not fuel-starved: all have central hot gas densities exceeding 10^{-25} gm cm^{-3}. Adopting masses from the $M_{\rm SMBH} - \sigma$ correlation, and assuming that mass is inflowing at the Bondi (1952) rate, we derive 3σ 2–10 keV luminosity upper limits of 7.3, 15 and $28 \times 10^{-9} L_{\rm Edd}$ and radiative efficiencies in this band of 4.1, 24, and 620×10^{-6} for NGC 1399, NGC 4472, and NGC 4636, respectively. Unless the black hole masses are considerably lower than predicted by the $M_{\rm SMBH} - \sigma$ correlation, these observations are inconsistent with the simplest ADAF models in NGC 1399 and NGC 4472, and imply accretion onto the SMBH at below the Bondi rate.

If the decline in the accretion rate is due to outflow, this raises the question of the ultimate fate of this gas as it encounters the dense hot interstellar medium in the core. Many questions about stability, intermittency, and regulation of gas flows in the inner regions of ellipticals remain to be addressed. The *Chandra* isophotes in the cores of NGC 1399 and NGC 4472 appear round and undisturbed, although there is an apparent spiral-like structure in the NGC 4636 diffuse emission.

The more stringent limits required to further constrain the nature of the central accretion flow will be difficult. Our observations indicate > 0.01 super-Eddington X-ray binaries per square-arcsecond near the nucleus; so that detections below $\sim 10^{39}$ erg s^{-1} cannot be unambiguously identified as AGN. Although the hot gas emissivity precipitously declines at energies above 2 keV, so does the *Chandra* sensitivity, restricting the detection limit in gas-rich systems. Tighter limits can be obtained on gas poor systems that, although of interest, may be fuel-starved and would thus shed little light on the accretion process. It would be especially useful to spectrally decompose the inner $\sim 1''$ to place a limit on the fraction of non-ISM emission. This would appear as a hard excess and would require a very deep exposure due to the declining *Chandra* effective area mentioned above.

We are grateful to Dave Davis and Una Hwang for assistance with data reduction, and to Wayne Landsman for sharing unpublished *HST* results. We made use of the *HST* archive, the NASA/IPAC Extragalactic Database (NED), and IDL function fitting routines developed by Craig Markwardt.

REFERENCES

Allen, S. W., Di Matteo, T., & Fabian, A. C. 2000, MNRAS, 311, 493

Angelini, L., Loewenstein, M. & Mushotzky, R. F. 2001, ApJ, submitted

Baganoff, F. K., et al. 2001, ApJ, submitted

Barger, A. J., Cowie, L. L., Mushotzky R. F., & Richards, E. A. 2001, AJ, 121, 662

Blandford, R. D., 1999, in ASP Conf. Ser. 182, ed. D. R. Merritt, M. Valluri, and J. A. Sellwood (San Francisco: ASP), 87

Blandford, R. D., & Begelman, M. C. 1999, MNRAS, 303, L1

Bondi, H. 1952, MNRAS, 112, 195

Brighenti, F., & Mathews, W. G. 1999, 527, L89

Ciotti, L. & Ostriker, J. P. 1997, ApJ, 487, L105

Di Matteo, T., Carilli, C. L., & Fabian, A. C. 2001, ApJ, 547, 731

Di Matteo, T., Fabian, A. C., Rees, M. J., Carilli, C. L., & Ivison, R. J. 1999, MNRAS, 305, 492

Di Matteo, T., Johnstone, R. M., Allen, S. W., & Fabian, A. C. 2001, ApJ, 550, L19

Di Matteo, T., Quataert, E., Allen, S. W., Narayan, R., & Fabian, A. C. 2000, MNRAS, 311 493

Fabian, A. C., & Iwasawa, K. 1999, MNRAS, 303, L34

Fabian, A. C., & Rees, M. J. 1995, MNRAS, 277, L55

Gammie, C. F., Narayan, R. & Blandford, R. D. 1999, ApJ, 516, 177

Garcia, M. R., Murray, S. S., Primini, F. A., Forman, W. R., McClintock, J. E., & Jones, C. 2000, ApJ, 537, L23

Gebhardt et al. 2000a, ApJ, 539, L13

Gebhardt et al. 2000b, ApJ, 543, L5

Geherels, N. 1986, ApJ, 303, 336

George, I. M., Mushotzky, R. F., Yaqoob, T., Turner, T. J., Kraemer, S., Ptak, A. F., Nandra, K., Crenshaw, D. M., & Netzer, H. 2001, ApJ, in press

Ho, L. C., Filipenko, A. V., & Sargent W.L. 1997, ApJ, 487, 568

Ho, L. C., et al. 2001, ApJ, in press

Loewenstein, M., Hayashida, K., Toneri, T., & Davis, D. S. 1998, ApJ, 497, 681

Magorrian et al. 1998, AJ, 115, 2285

Mahadevan, R. 1997, ApJ, 477, 585

McLure & Dunlop, J. S. 2000, MNRAS, submitted

Merritt, D., & Ferrarese, L. 2001a, ApJ, 547, 140

Merritt, D., & Ferrarese, L. 2001b, MNRAS, 320, 30

Monet et al. 1998, USNO-A V2.0, A Catalog of Astrometric Standards (Flagstaff: U.S. Naval Observatory)

Mushotzky R. F., Cowie, L. L., Barger, A. J., & Arnaud, K. A. 2000, Nature, 404, 459

Narayan, R., Igumenshchev, I. V., & Abramowicz, M. A. 2000, ApJ, 539, 798

Narayan, R. & Yi, I. 1994, ApJ, 428, L13

Quataert, E., & Gruzinov, A. 1999, ApJ, 539, 809

Quataert, E., & Narayan, R. 1999, ApJ, 520, 298

Quataert, E., & Narayan, R. 2000, ApJ, 528, 236

Quataert, E., Narayan, R., & Reid, M. J. 1999, ApJ, 517, 101

Roberts, T. P., & Warwick, R. S. 2000, MNRAS, 315, 98

Sulkanen, M. E., & Bregman, J. N. 2001, ApJ, 548, L131

Table 1. Galaxy and Accretion Flow Characteristics

galaxy NGC	d Mpc	$M_{\rm SMBH}$ 10^8 $M_\odot$	$R_{\rm Bondi}$ $''$	$\dot{M}_{\rm Bondi}$ $M_\odot$ yr^{-1}	$L_{\rm edd}$ erg s^{-1}	$L_{\rm Bondi}$[a] erg s^{-1}	$L_{\rm ADAF}$[b] erg s^{-1}	L_X[c] erg s^{-1}	L_X[d] erg s^{-1}
1399	20.5	10.6	0.36	$4.0\ 10^{-2}$	$1.3\ 10^{47}$	$2.3\ 10^{44}$	$2\ 10^{41}$	$< 9.7\ 10^{38}$	$< 9.7\ 10^{38}$
4472	16.7	5.65	0.24	$7.9\ 10^{-3}$	$7.1\ 10^{46}$	$4.5\ 10^{43}$	10^{40}	$< 6.4\ 10^{38}$	$< 4.9\ 10^{38}$
4636	15.0	0.791	0.049	$8.0\ 10^{-5}$	$9.9\ 10^{45}$	$4.5\ 10^{41}$	10^{36}	$< 2.7\ 10^{38}$	$< 1.8\ 10^{38}$

[a] $0.1\dot{M}_{\rm Bondi}c^2$

[b] approximate expectation of standard ADAF model; see text

[c] 2–10 keV upper limit from this paper for $3''$ box

[d] 2–10 keV upper limit at assumed optical nucleus

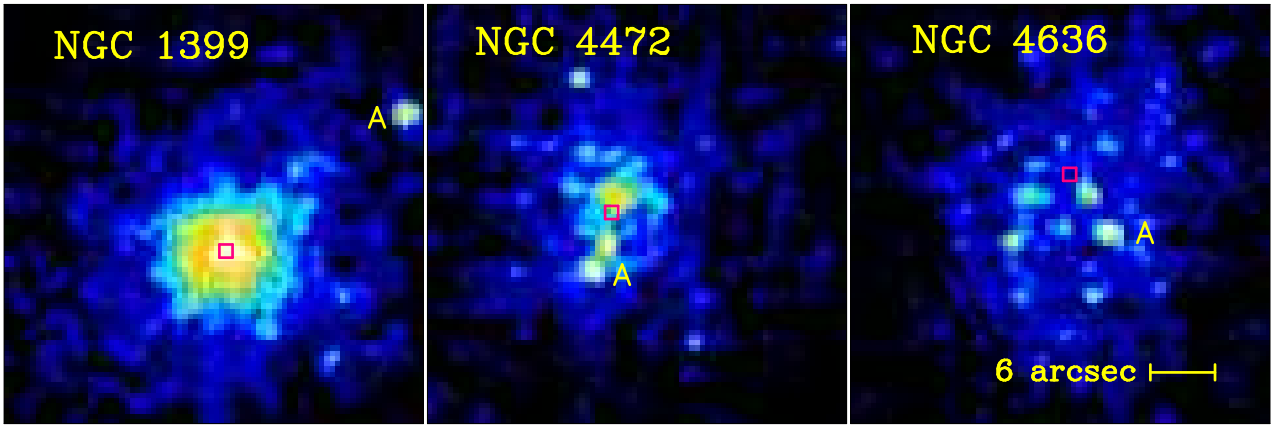

Fig. 1.— *Chandra* ACIS-S3 1.25–7 keV images of the central $50'' \times 50''$ of (a) NGC 1399, (b) NGC 4472, and (c) NGC 4636. The open, $1'' \times 1''$ box indicates the position of the optical (*HST*) nucleus, the letter "A" the brightest point source. Relative shifts based on image registration have been applied for NGC 1399 (1.5″)and NGC 4636 (0.9″).

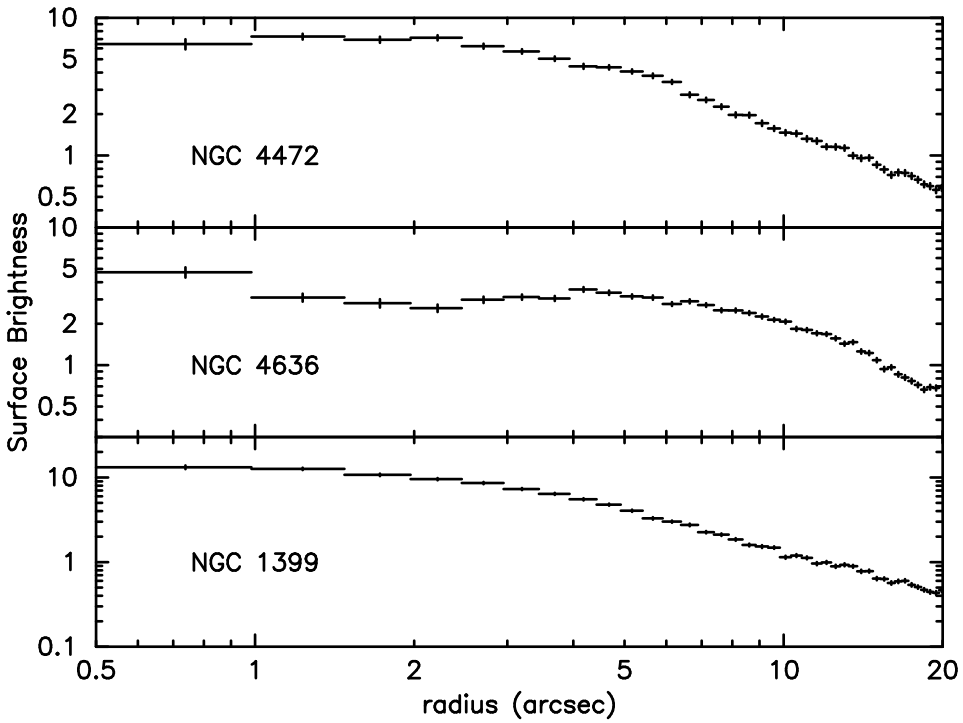

Fig. 2.— *Chandra* ACIS-S3 0.3–7 keV central diffuse emission surface brightness distributions in cts arcmin^{-2} s^{-1}. Annuli are centered on the X-ray centroids for NGC 1399 and NGC 4472, and on the near nuclear source for NGC 4636.